Research reports from undergraduate students receiving support from the Shackouls Honors College via the Summer Research Fellowship

Spring 2023

Director:
Dr. Anastasia Elder

Edited by:
Elizabeth Fox

Table of Contents

Name: Austen Breland

Faculty Mentor: Dr. Steven H. Elder

Department: Agricultural and Biological Engineering

Introduction

My research this semester focused on the development of a viable long-term drug delivery system for osteoarthritis (OA) treatment using punicalagin (PCG) as the active pharmaceutical compound. OA is a chronic, degenerative disease that affects millions of Americans. This condition involves the gradual degradation of articular cartilage that covers the end of long bones in joints like the knee. OA is associated with pain, stiffness, swelling, and loss of range of motion in the affected joint. The most prevalent articularly-injected treatment methods for OA, corticosteroids and hyaluronic acid, only temporarily reduce symptoms with no long-term delay in the progression of OA. PCG is a phenolic compound that is commonly found in pomegranates. Polyphenols, such as PCG, are commonly heralded for a wide range of health benefits centering around their potent antioxidant capabilities, with little concern for localized or systemic cytotoxicity. PCG has been previously demonstrated to provide collagen with increased resistance to enzymatic degradation via collagenase and hyaluronidase. Therefore, it shows promise as a potential preventative treatment for osteoarthritis progression. However, further research is necessary to better understand the chondroprotective properties of PCG.

Experiment 1: Analysis of Punicalagin's Effect on Cartilaginous Aggrecan Degradation via ADAMTS-5

Background

ADAMTS-5 is a principal destructive enzyme in the progression of OA and is the main enzyme involved in the breakdown of the cartilage extracellular matrix (ECM) via the extraction of aggrecan, the main proteoglycan in collagen. Aggrecan consists of keratin sulfate and chondroitin sulfate glycosaminoglycan (GAG) bound to a protein core (Figure 1) [1]. Within cartilage, aggrecan monomers are attached to hyaluronic acid chains via link proteins. This structure provides cartilage with compressive stiffness by increasing the fluid pressure within the cartilage via the dense negative charge on GAG chains [2]. The removal of aggrecan via ADAMTS-5 increases the stress placed on cartilage, increasing inflammation and accelerating the progression of OA. Therefore, OA treatment methods that inhibit the effects of ADAMTS-5 provide promise for actively slowing the progression of the disease.

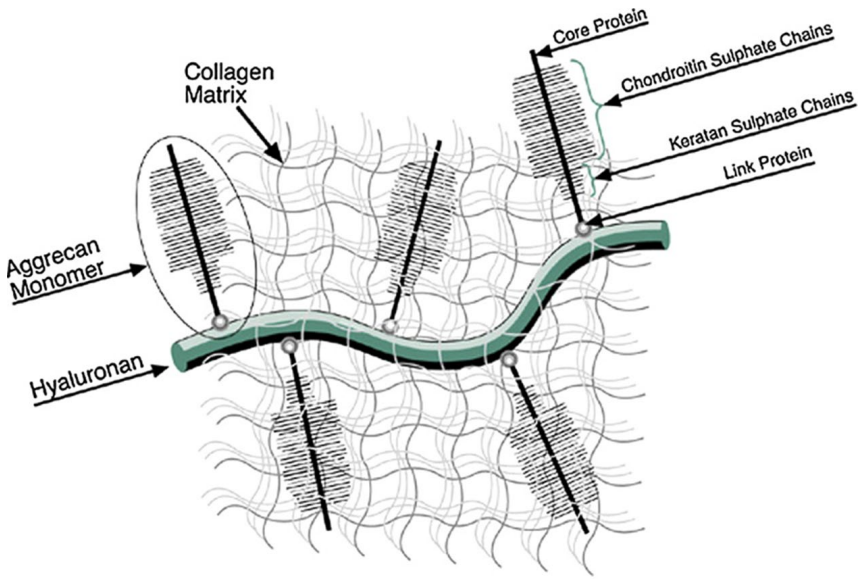

Figure 1. Cartilage Extracellular Matrix

Methods and Materials

This experiment sought to determine the potential inhibitory effects of PCG on ADAMTS-5. To do so, an *in vitro* model of porcine cartilage explants was used. Ø5 mm decellularized, freeze-dried porcine articular cartilage disks obtained from stifle joint using a biopsy punch. 24 cartilage explants were individually massed and placed in 1.5 mL microcentrifuge tubes. Human recombinant ADAMTS-5 was then dissolved at a concentration of 0.4 µg/mL in a 50 mL of 50 mM Tris, 100 mM NaCl, 5 mM $CaCl_2$, 0.05% Tween-20 buffer solution, which was then adjusted to a pH of 7.5. 750 µL of this enzyme buffer was transferred to each of the 24 microcentrifuge tubes holding the cartilage explants. 100 µM of PCG was then added to 12 of the microcentrifuge tubes. All the microcentrifuge tubes were kept in an orbital shaker at 100 RPM and 37 °C. 6 explants (3 from the PCG treated group, 3 from the non-treated group) were collected every three days and frozen to prevent further degradation. The buffer solution and PCG were then replaced, with the same explants receiving the PCG treatment for the entire duration of the experiment. After a total of 12 days, all the collected explants were freeze-dried and re-massed. The explants were each then digested overnight in 1 mL of a solution containing 5 µL papain and 1.58 mg L-cysteine at 60 °C. The homogenous papain solution was then diluted at a 1:15 ratio with PBE. A sulfated GAG dimethyl methylene blue assay kit was finally used to quantify the remaining GAG mass in the digested explants.

To quantify the relative percentage of GAG loss after each period of exposure indicated by the sulfated GAG assay, three additional explants were massed before being digested overnight in an identical cysteine-activated papain buffer. However, the unexposed explants were necessarily diluted at a 1:75 ratio due to the concentration of GAG exceeding the range that is accurately measured by the GAG assay (1-5 µg/mg).

Results

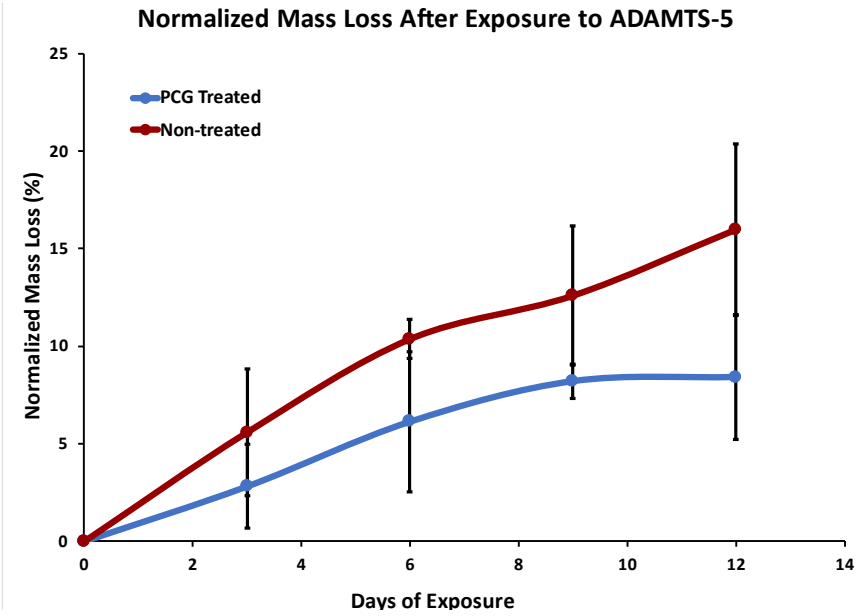

Figure 2. Time Dependent Mass Loss

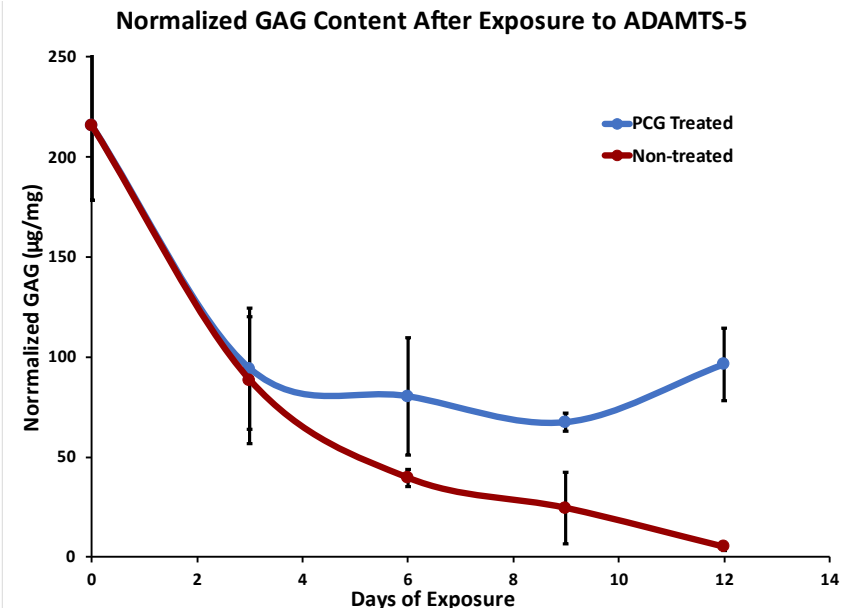

Figure 3. Time Dependent GAG Loss

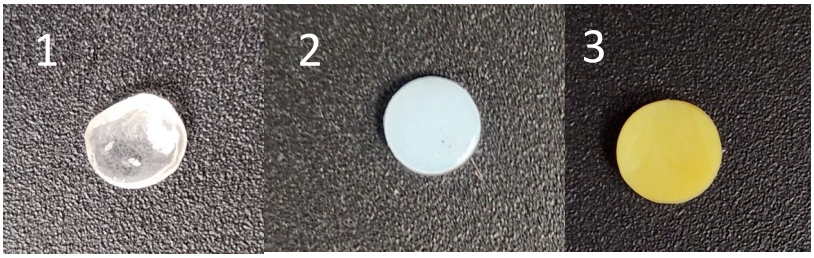

Figure 4. (1) Freeze-dried cartilage explant, (2) hydrated cartilage explant, (3) punicalagin treated cartilage explant

Figure 2 displays the recorded mass loss after exposure to the ADAMTS-5 buffer. The recorded loss represents the percentage of original mass lost after each specific period of exposure. The average percent loss of the triplicate samples collected from both the treated and non-treated groups were averaged together, and this average was recorded along with the standard deviation of the triplicate group. Treatment with PCG significantly decreased the mass loss at each interval. After 12 days of exposure, samples lost an average of 8.42% compared to 15.98% lost by non-treated samples.

Figure 3 depicts the results of the sulfated GAG assay. The normalized concentration of GAG remaining in the triplicate samples collected at each interval were averaged together. The concentration of GAG in the unexposed explants is much greater than that previously depicted in literature, so it likely does not give an optimal demonstration of the relative GAG loss of both the treated and non-treated groups. While the concentration of GAG in the unexposed explants during this experiment averaged 215.6 µg/mg, the concentration of porcine cartilage explants has previously been shown to average 94.1 µg/mg [3]. Since the concentration of GAG in cartilage varies significantly with depth from the articular surface, it is believed that the variance seen in the results of this experiment is due to inconsistent depth of explant extraction. However, the results of the sulfated GAG assay still indicate that treatment with PCG significantly reduced the GAG loss experienced due to exposure to ADAMTS-5. After 12 days, the GAG remaining in the PCG-treated group was 96.3 µg/mg and the concentration of the non-treated group was 5.1 µg/mg. When compared to the concentration of the unexposed explants analyzed during this experiment, the remaining GAG after 12 days of exposure represents a 55.3% loss in the group treated with PCG and a 97.6% loss in the non-treated group. Interestingly, if the results are compared to the concentration of GAG previously demonstrated, treatment with PCG entirely eliminates GAG loss due to ADAMTS-5. This gives strong evidence for PCG being an active inhibitor of ADAMTS-5, which gives greater promise for its potential as an effective treatment of OA.

Experiment 2: Molecular Docking for the Simulation of Punicalagin's Mechanism of Action in the Inhibition of ADAMTS-5

Background

Metalloproteinases are a class of enzymes that degrade ECM components. A disintegrin-like and metalloprotease domain with thrombospondin type 1 repeats (ADAMTS) metalloproteinases are integral in the progression of many chronic diseases, including OA [4]. Aggrecanases are a subset of metalloproteinases that act directly on aggrecan in the ECM by cleaving it. ADAMTS-5 (aggrecanase-2) is known to participate in cartilage degradation by cleaving the GLU373-ALA374 bond of aggrecan [4]. From the analysis of crystallographic structures, inhibitors of ADAMTS-5 are known to bind within the S_1 and S'_1 domains of ADAMTS-5 [5]. These domains form a characteristic fold that facilitates the coordination of a zinc ion. The pocket of the active site in ADAMTS-5 is defined by HIS410, HIS414, and HIS420, with GLU411 also being involved in binding to zinc ions. This pocket is seen depicted in Figure 6. Figure 7 depicts the interactions of a known inhibitor, GLPG192/S201086 (PDB ID 38BZ), with this pocket, preventing the cleavage of aggrecan via ADAMTS-5 [5]. These figures were made with the use of ProteinPlus, a University of Hamburg structure-based modeling support server. 2D interaction diagrams utilize conventional chemical drawing visualizations, with H-bonding represented by dashed black lines and hydrophobic interactions represented by green splines.

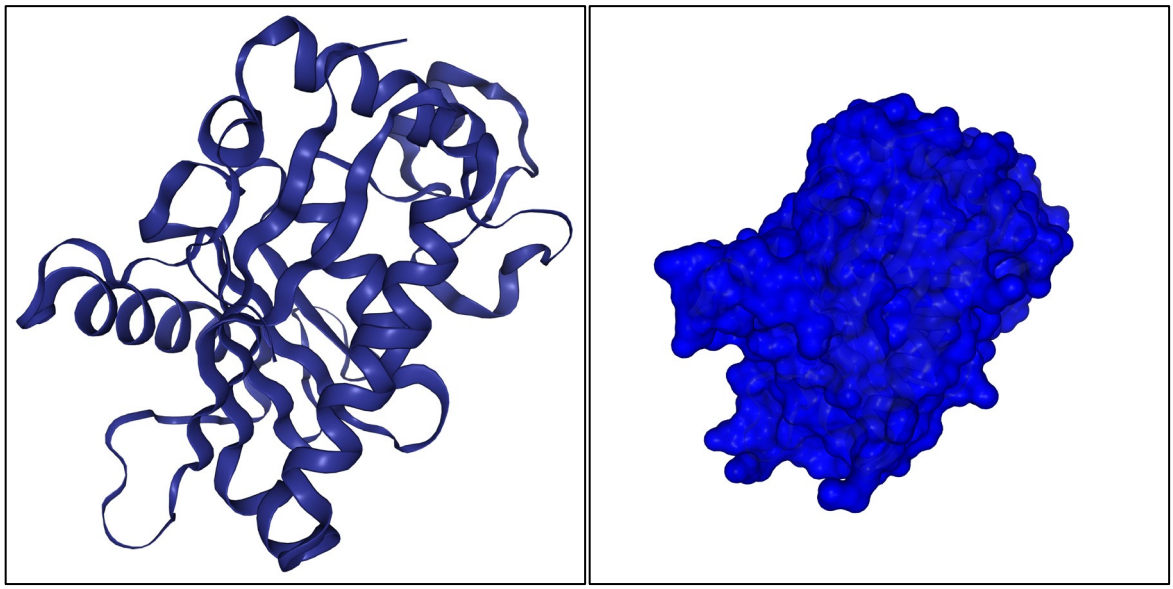

Figure 5. ADAMTS-5 Structure

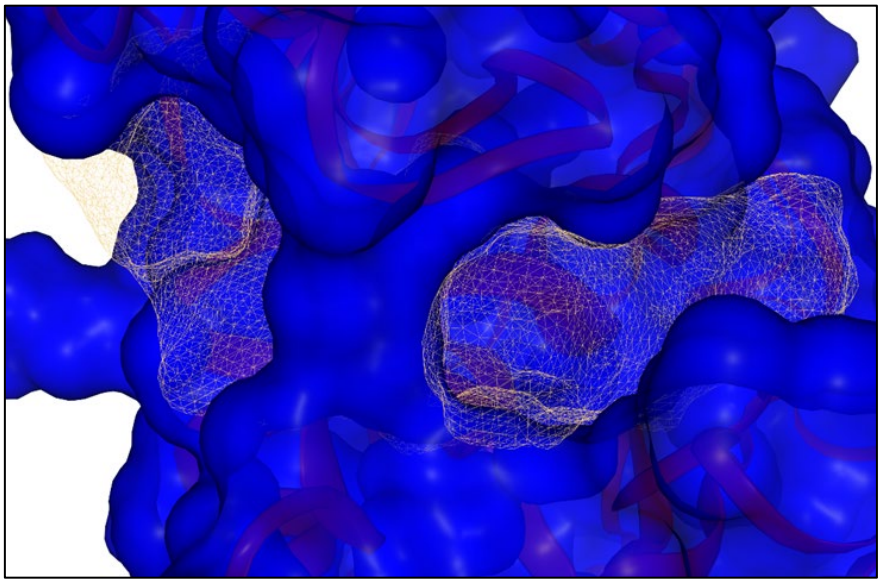

Figure 6. ADAMTS-5 Active Site

AutoDock is a tool that allows the prediction of interactions between ligands and biomolecules, often referred to as molecular docking. AutoDock utilizes the Lamarckian Genetic Algorithm and an empirical scoring function to predict ligand-molecule conformations that minimize the interaction energy required to produce them [6]. The combination of these allows possible ligand binding conformations to be selectively eliminated based on their likelihood of occurrence. During this experiment, AutoDock Tools (ADT) was used to predict potential ligand binding conformations of PCG and its metabolic derivatives within the active site of ADAMTS-5. Hexahydroxydiphenic (HHDP) acid, d-glucose, and gallagic acid (GA) were determined to be likely metabolic derivatives of PCG due to the susceptibility of ester linkage hydrolysis in biological environments as well as the prevalence of ester bond cleavage via protease activity [7,8]. However, HHDP acid is an unstable structure that is spontaneously converted to Ellagic acid (EA) via lactonization [9]. These degradation pathways can be seen as illustrated in Figure 8.

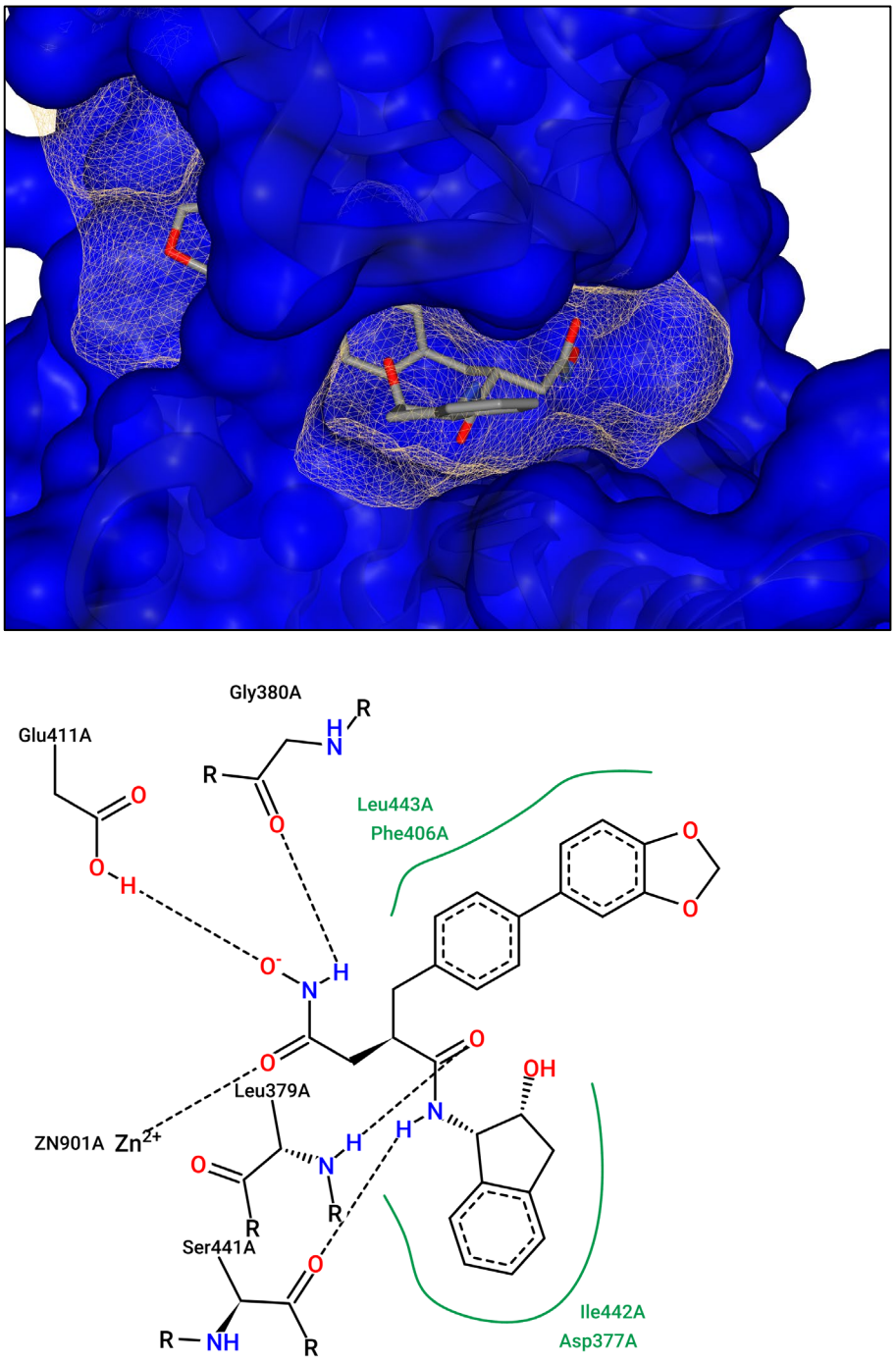

Figure 7. (Top) ADAMTS-5 Inhibitor binding to active site, (Bottom) 2D inhibitor interaction diagram

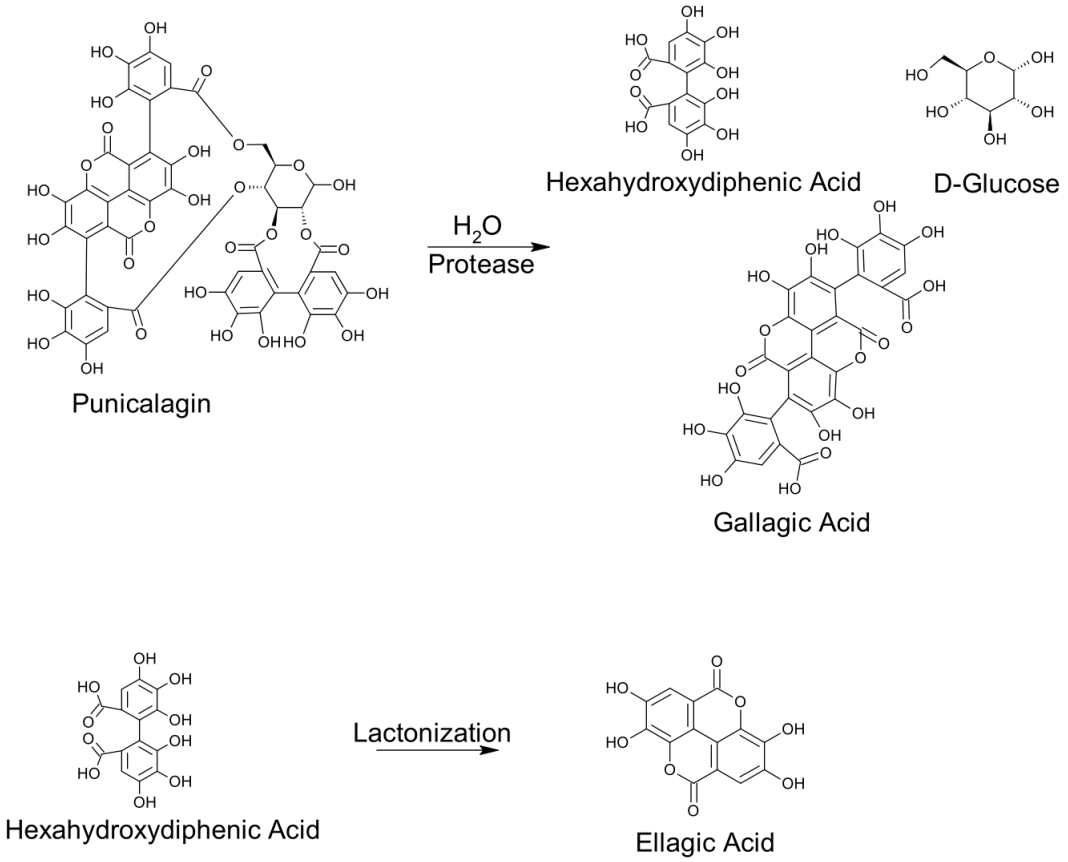

Figure 8. Punicalagin Degradation Pathway

Materials and Methods

Using molecular docking simulations, the following ligands were each used individually to predict potential binding conformations: PCG, EA, HHDP acid, and GA. The 3D structures for these ligands were each downloaded from PubChem in .sdf format, with the only exception being PCG. Due to its large molecular weight, the structure for PCG was downloaded from MolView in .mol format. The structure of ADAMTS-5 was downloaded from the Protein Data Bank (PDB) in .pdb format using ID 3LJT.

The .pdb structure of ADAMTS-5 was first imported through “File > Read Molecule.” All water molecules were then removed from the structure using “Edit > Delete Waters.” The ligand and bound ions were then removed by selecting these atoms in the Dashboard and using “Edit > Delete > Delete Selected Atoms.” This was followed by “Edit > Misc > Repair Missing Atoms.” The missing hydrogens were then added through “Edit > Hydrogens > Add” with the inputs in Figure 9.

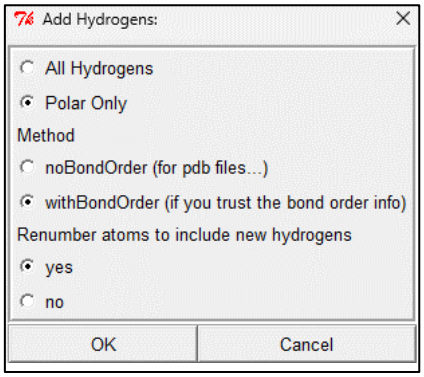

Figure 9. Hydrogen Inputs

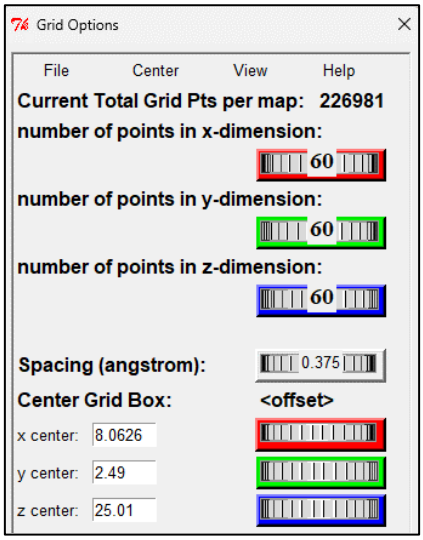

Figure 10. Grid Box Inputs

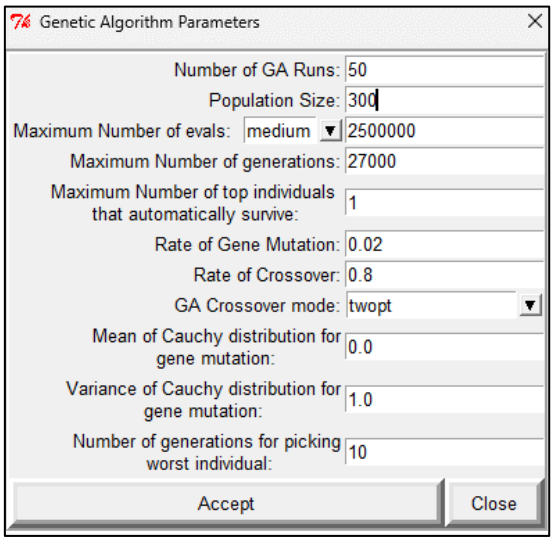

Figure 11. Algorithm Parameter Inputs

Relevant charges were then added to the structure using "Edit > Charges > Add Kollman Charges." These charges were evenly distributed using "Edit > Charges > Check Totals on Residues > Spread Charge Deficit > Dismiss."

The .sdf structure of the ligand was then imported using "Ligand > Input > Open" and saved as a .pdbqt file using "Ligand > Output."

After importing the ligand, the grid maps were developed. The grid maps are 3D matrices of evenly distributed points used to determine the potential binding energy for the ligand within a region of interest. "Grid > Macromolecule > Choose" was used to select the enzyme structure and "Grid > Set Map Types > Choose" was used to select the ligand structure for each simulation. The grid box defines the region of ADAMTS-5 where docking simulations will be administered within. This was defined using "Grid > Grid Box" using the parameters in Figure 10 followed by selecting "File > Close Saving Current." The 3D dimensional coordinates used to define the center of the grid box were chosen as the average of the 3D coordinates of the first atom for 6 residues (L402, H403, A404, H410, R437, I446) that form the active site of ADAMTS-5. The parameters used to develop the grid box were saved using "Grid > Output > Save GPF." Finally, the grid map files were created by using "Run > Run AutoGrid," inputting the relevant file paths for the program and parameter files, and selecting "Launch."

The parameter files for docking were the final requirement before simulating ligand binding to the enzyme. The enzyme and ligand structures were again selected using "Docking > Macromolecule > Set Rigid Filename" and "Docking > Ligand > Choose." The algorithm parameters were determined by using "Docking > Search Parameters > Genetic Algorithm" and inputting the parameters in Figure 11. The docking parameters were saved using "Docking > Output > Lamarckian GA." The docking simulations were then performed using "Run > Run AutoDock," inputting the file paths for the program and parameter files, and launching.

Results

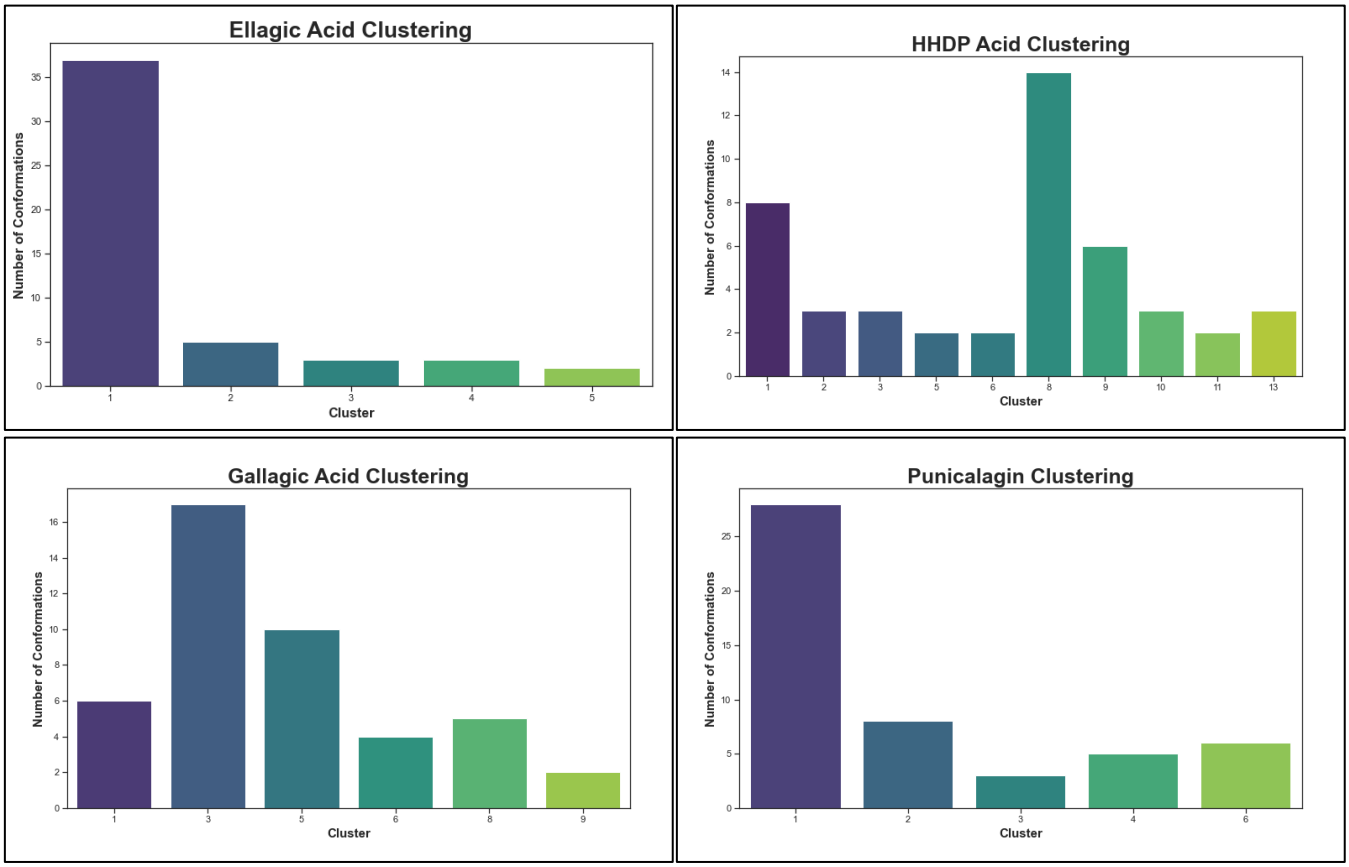

Figure 12. Clustering of molecular docking enzyme-ligand conformations

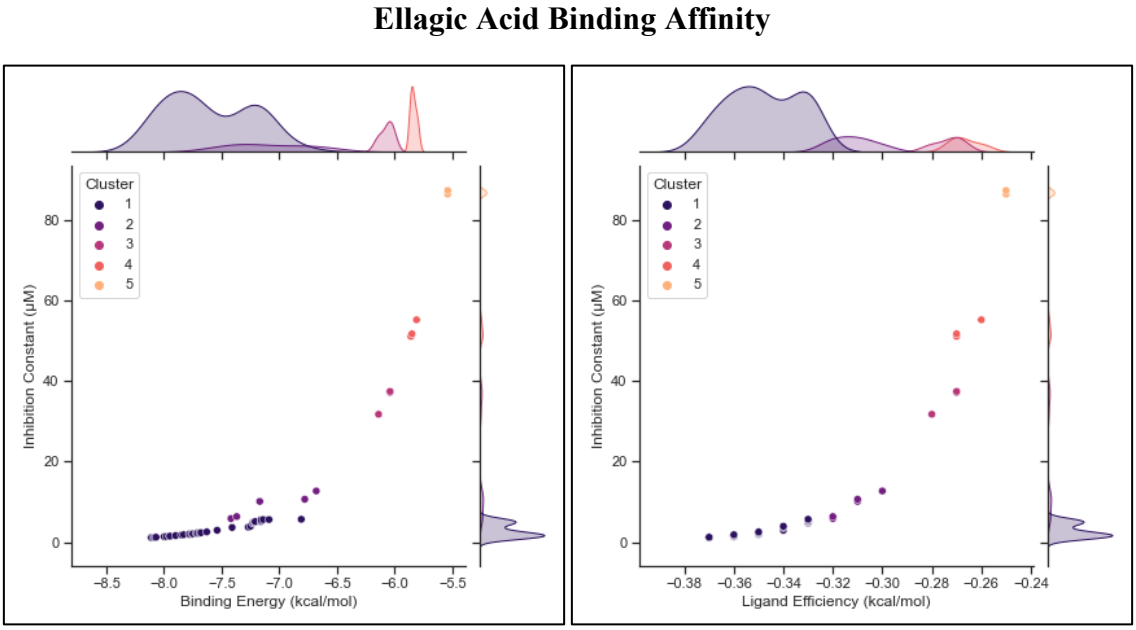

Figure 13. Simulated binding affinity between ADAMTS-5 and EA

HHDP Acid Binding Affinity

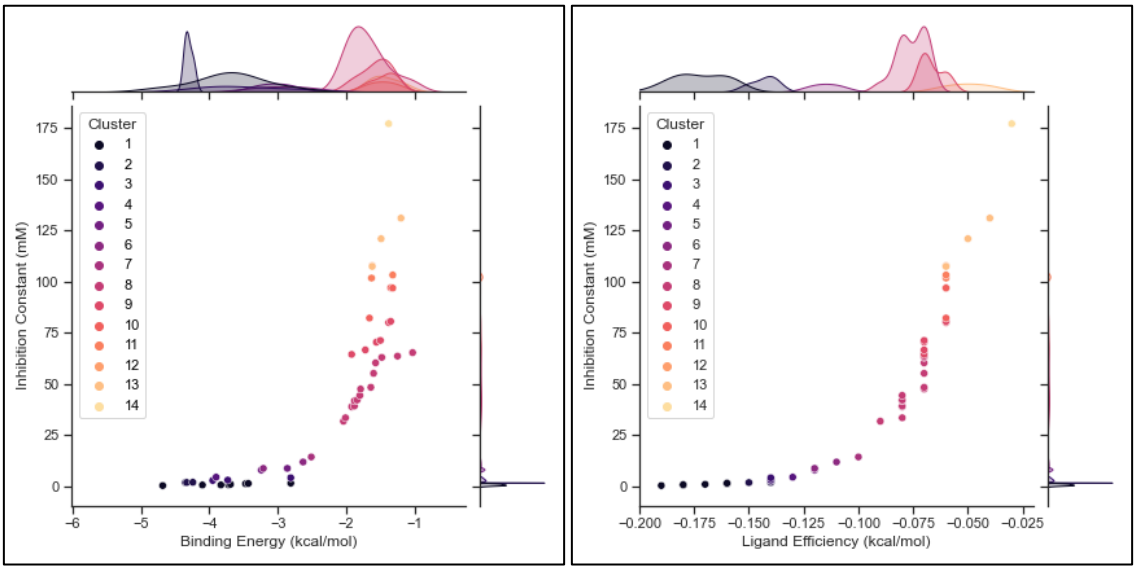

Figure 14. Simulated binding affinity between ADAMTS-5 and HHDP acid

Gallagic Acid Binding Affinity

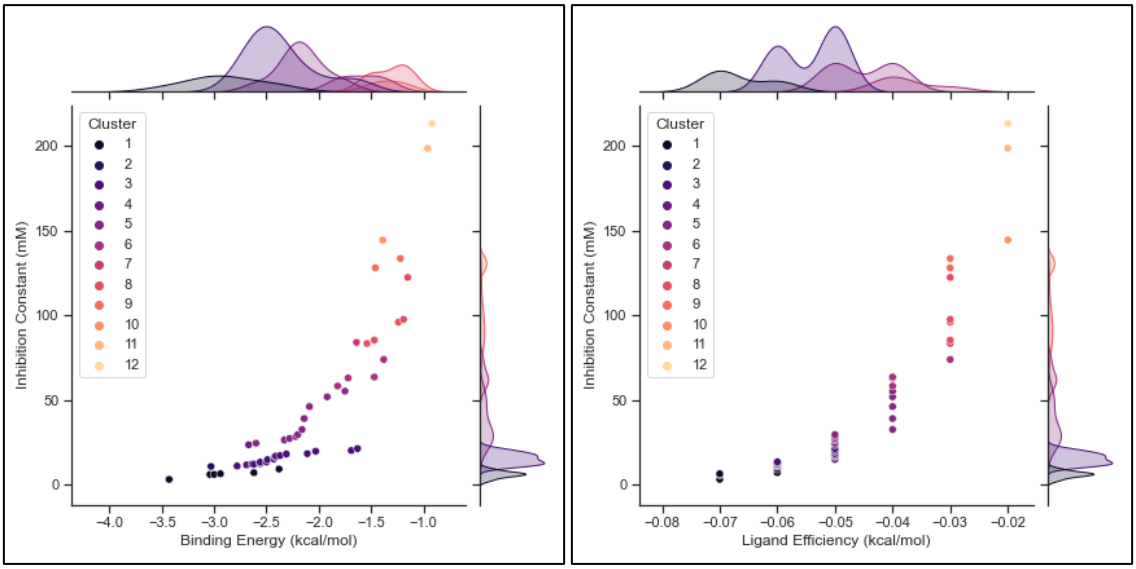

Figure 15. Simulated binding affinity between ADAMTS-5 and GA

Punicalagin Binding Affinity

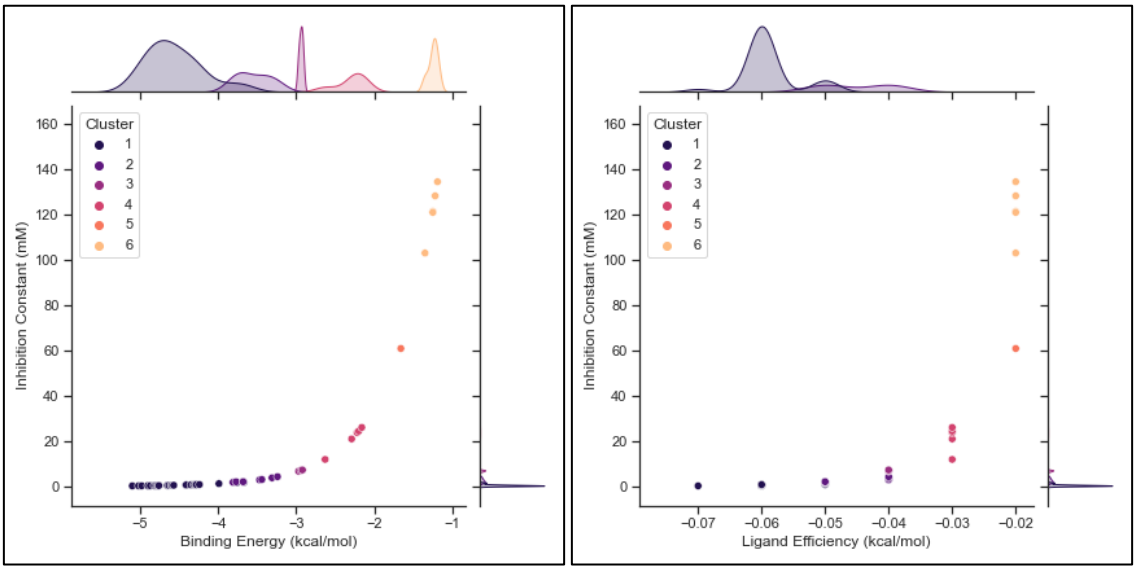

Figure 16. Simulated binding affinity between ADAMTS-5 and PCG

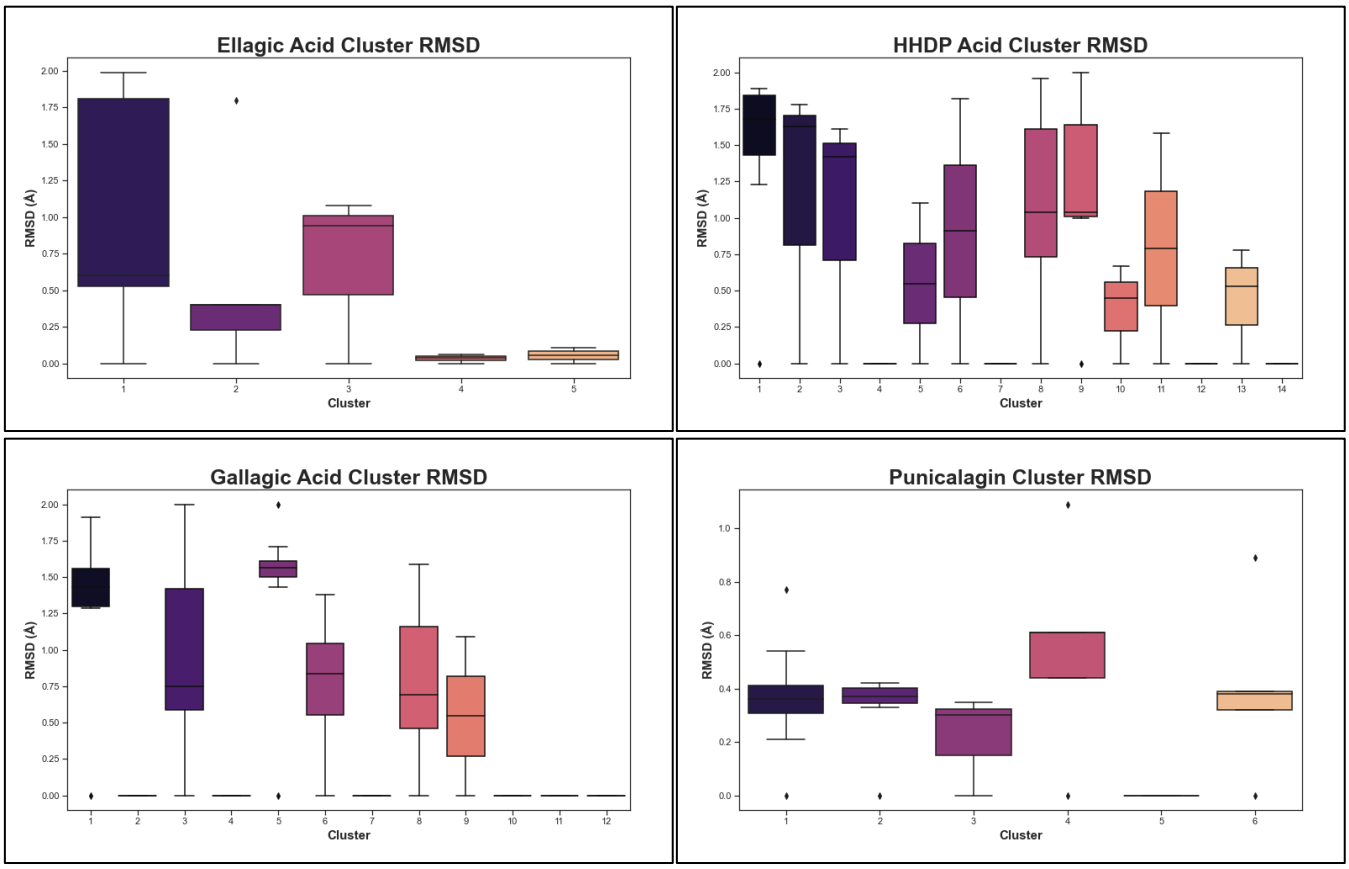

Figure 17. RMSD (Å) of enzyme-ligand conformation clusters

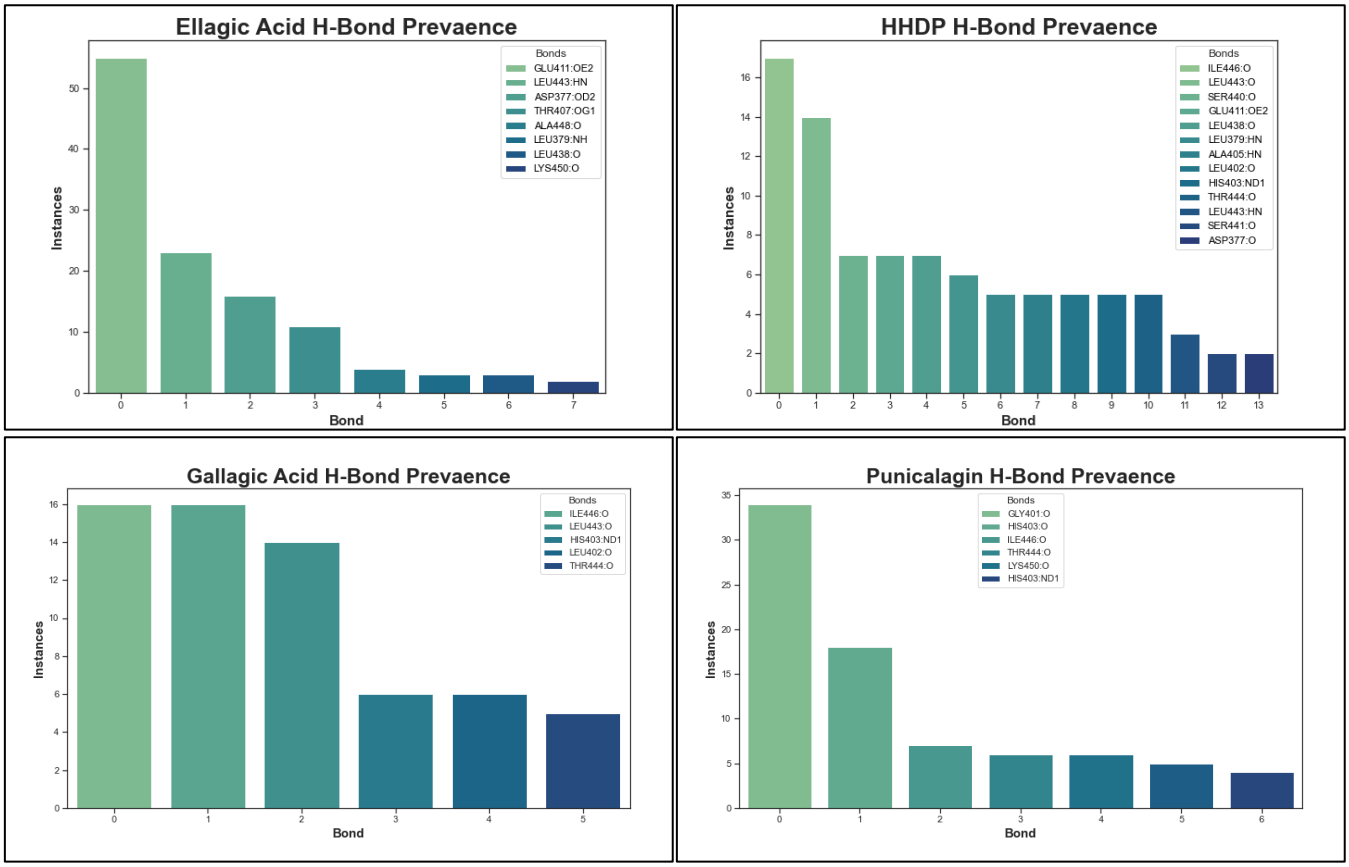

Figure 18. Prevalence of H-bonds formed across all enzyme-ligand conformations

Parameter	Ellagic Acid			HHDP Acid		
	extremum	Mean	SD	extremum	Mean	SD
Binding Efficiency (kcal/mol)	-0.37	-0.348	0.0144	-0.09	-0.0757	0.00646
Binding Energy (kcal/mol)	-8.11	-7.61	0.369	-2.04	-1.7	0.29
Inhibition Constant (µM)	1.13	2.97	1.64	31810	48232.14	11406.53
Parameter	Gallagic Acid			Punicalagin		
	extremum	Mean	SD	extremum	Mean	SD
Binding Efficiency (kcal/mol)	-0.06	-0.0541	0.00507	-0.07	-0.589	0.00416
Binding Energy (kcal/mol)	-2.78	-2.37	0.327	-5.1	-4.56	0.357
Inhibition Constant (µM)	10950	15485.88	3269.41	183.34	541.02	388.46

Table 1. Analysis of binding affinity for most prevalent cluster of each enzyme-ligand combination

Each AutoDock simulation resulted in 50 potential enzyme-ligand conformations for each enzyme-ligand combination. These 50 conformations were organized into clusters based on the similarity of their binding location, which can be seen in Figure 12. Due to molecular docking's bias towards false positive results, the purpose of these clusters is to analyze whether each enzyme-ligand simulation converged toward an optimal structure. This convergence is seen in many conformations belonging to a single cluster. The variance within clusters was analyzed using root-mean-square deviation (RMSD) among the conformations found within each cluster. Lower RMSD signifies lower variance in the ligand's bond angles and atom positions, with a value below 2.0 Å considered good. These RMSD values are reported in Figure 17. None of the resulting conformations exhibited an unacceptable RMSD value, which indicates a higher resolution.

The binding affinity of each enzyme-ligand combination was also analyzed using the predicted binding energy (kcal/mol), ligand efficiency (kcal/mol), and inhibition constant (μM). These results are displayed in Figures 13-16. EA displayed significantly lower binding energy, ligand efficiency, and inhibition constant when compared to the other ligands analyzed during this experiment. These metrics indicate that EA is most likely to actively inhibit the effects of ADAMTS-5 by binding directly to the active site. A statistical analysis of the binding energy, ligand efficiency, and inhibition constant for the most prevalent cluster of each enzyme-ligand combination makes this result more apparent. To further analyze the potential inhibitory mechanism of action of EA. The lowest energy binding conformation (binding energy = -8.11 kcal/mol) was further analyzed by identifying the specific enzyme-ligand interactions. These interactions can be seen visualized in Figure 19, with H-bonds displayed as green dashed lines with their corresponding bond lengths and hydrophobic interactions displayed as red dashed lines. The binding location of EA within the active site of ADAMTS-5 can also be seen in Figure 19.

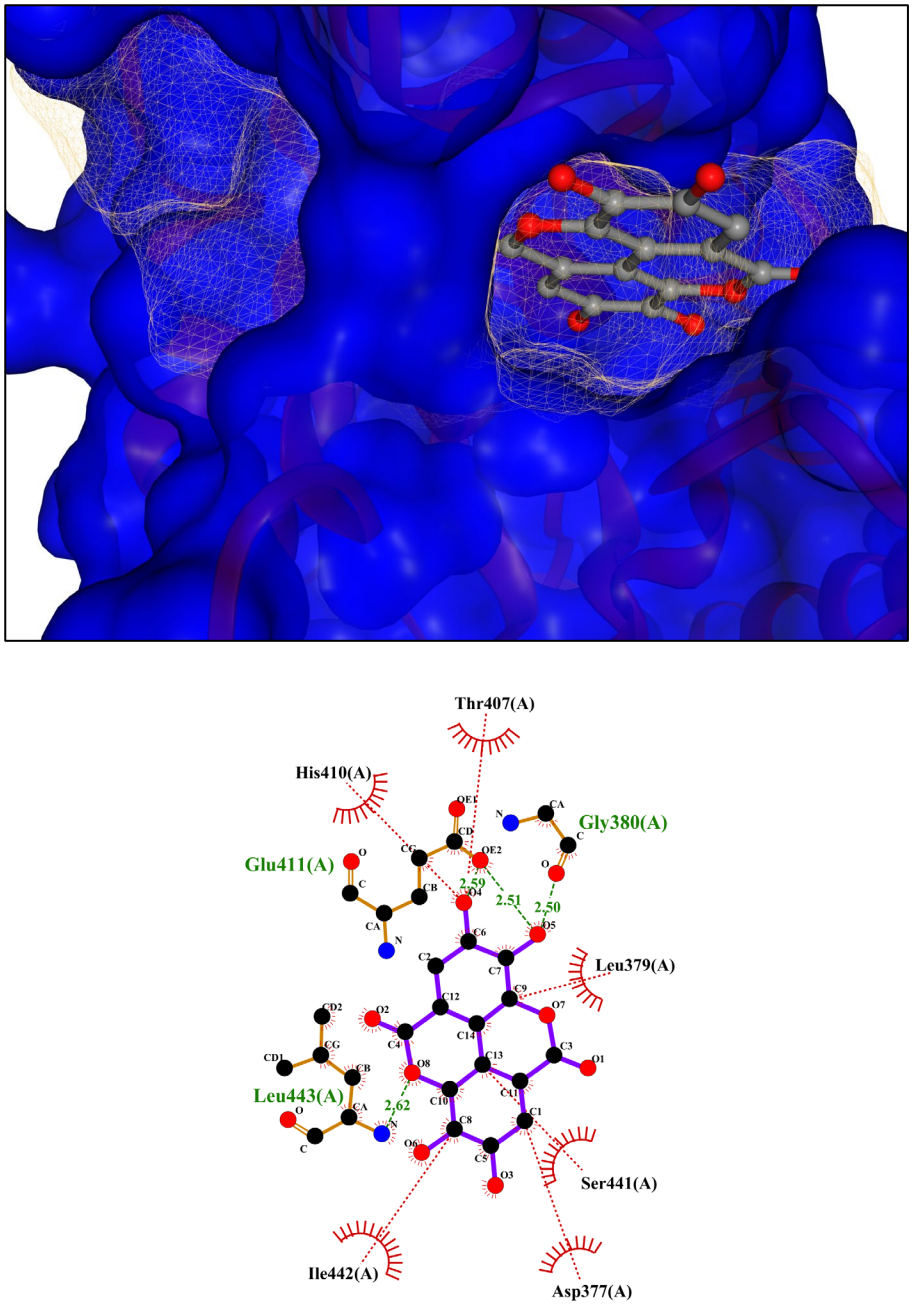

Figure 19. (Top) EA binding to active site, (Bottom) 2D EA interaction diagram

Conclusion

The removal of aggrecan in articular cartilage by ADAMTS-5 is effectively inhibited by PCG. To the authors' knowledge, this is the first instance of PCG being demonstrated to inhibit ADAMTS-5. This discovery significantly contributes to the potential for PCG to be used in the treatment of OA. In biological conditions, PCG likely metabolized to form HHDP acid, GA, and d-glucose via the hydrolysis of ester linkages. HHDP acid is also further degraded into EA, which has the greatest potential to directly bind to the active site of ADAMTS-5, via the lactonization of adjacent hydroxyl groups. The binding of EA within the active site of ADAMTS-5 prevents the binding of aggrecan, which actively inhibits the enzyme's role in the progression of OA. The binding of EA within the active site of ADAMTS-5 is primarily facilitated by the formation of H-bonds between the hydroxyl groups of GLU411 and EA, between the amino group of LEU443 and a pyran O of EA, and between the carbonyl O of GLY380 and a hydroxyl group of EA. This binding is also supported by hydrophobic interactions between EA and the following residues of ADAMTS-5: THR407, HIS410, LEU379, ILE442, ASP377, and SER441. These interactions align with the ligand-enzyme interactions of a known inhibitor, GLPG192/S201086. This further lends credibility to EA being the active pharmaceutical component in PCG's inhibition of ADAMTS-5.

Further work will be undertaken to determine if treatment with isolated EA will inhibit aggrecan degradation in a similar manner to PCG treatment. Additionally, the presence of EA in solution, as well as the other hypothesized PCG metabolized, will be analyzed to confirm that the proposed metabolic degradation of PCG is accurate. Following these steps, a dose-dependent relationship between EA and ADAMTS-5 inhibition will be developed to examine the sensitivity of EA's inhibitory activity. This knowledge will further define the function of PCG as well as its metabolites in mediating the progression of OA.

References

1. van Weeren, P. R. & Firth, E. C. Future Tools for Early Diagnosis and Monitoring of Musculoskeletal Injury: Biomarkers and CT. *Veterinary Clinics of North America - Equine Practice* **24**, 153–175 (2008).

2. Kiani, C., Chen, L., Wu, Y. J., Yee, A. J. & Yang, B. B. Structure and function of aggrecan. *Cell Res* **12**, 19–32 (2002).

3. Elder, S. *et al.* Effects of antigen removal on a porcine osteochondral xenograft for articular cartilage repair. *J Biomed Mater Res Part A* **106**, 2251–2260 (2018).

4. Li, T. *et al.* The Mechanism and Role of ADAMTS Protein Family in Osteoarthritis. *Biomolecules 2022, Vol. 12, Page 959* **12**, 959 (2022).

5. Brebion, F. *et al.* Discovery of GLPG1972/S201086, a Potent, Selective, and Orally Bioavailable ADAMTS-5 Inhibitor for the Treatment of Osteoarthritis. *J Med Chem* **64**, 2937–2952 (2021).

6. Morris, G. M. *et al.* User Guide AutoDock Version 4.2 Updated for version 4.2.6 Automated Docking of Flexible Ligands to Flexible Receptors. (1991).

7. Klein, P. *et al.* New Cysteine Protease Inhibitors: Electrophilic (Het)arenes and Unexpected Prodrug Identification for the Trypanosoma Protease Rhodesain. *Molecules 2020, Vol. 25, Page 1451* **25**, 1451 (2020).

8. Li, M., Rauf, A., Guo, Y. & Kang, X. Real-Time Label-Free Kinetics Monitoring of Trypsin-Catalyzed Ester Hydrolysis by a Nanopore Sensor. *ACS Sens* **4**, 2854–2857 (2019).

9. Aguilera-Carbo, A., Augur, C., Prado-Barragan, L. A., Favela-Torres, E. & Aguilar, C. N. Microbial production of ellagic acid and biodegradation of ellagitannins. *Appl Microbiol Biotechnol* **78**, 189–199 (2008).

Name: Miller, Hannah

Faculty Advisor: Dr. Richard Baird

Project Title: *Temporal Study of Reactive Oxygen Species in Two Soybean Cultivars*

Introduction:

This year, I worked with Dr. Baird and Hannah Purcha in Dr. Baird's lab in the Department of Biochemistry, Molecular Biology, Entomology, and Plant Pathology. We collaborated with Dr. Reddy, Plant and Soil Science Department, who was studying soybean plants growing in different environmental conditions including temperature variations, drought, and carbon dioxide levels all associated with climate change. Leaf samples from 240 soybean plants were removed that were part of their study grown in outside chamber system. My specific project involved running assays to measure the levels of reactive oxygen species (ROS) in the samples looking at intermediates associated with the antioxidant:oxidant ratios that if out of balance can cause cell damage. Our goal was to determine the effects of the various environmental stressors on ROS levels.

The Honors Research Fellowship supported my research endeavors by providing the salary for my hours working in the lab. This allowed me to focus more fully on the research and strengthen my laboratory skills. The skills I developed have helped me succeed in my upper-level biochemistry classes this semester and prepared me for my professional career by teaching me skills necessary to work in clinical and non-clinical lab settings. This fellowship also taught me how to manage my time effectively while performing the assays, which at times could be very time intensive. Lastly, presenting the research at the Undergraduate Research Symposium in April taught me how to prepare an informative poster and effectively communicate my research to others.

Materials and Methods:

For these experiments, we used four different ROS assays, supplied by Abcam: Glutathione Reductase, Glutathione Peroxidase, Lipid Peroxidation (MDA), and Hydrogen Peroxide. During the funding period of the fellowship, I focused on running the four protocols on soybean tissue collected from two different cultivars (DS25-1 and DS31-243) that were subjected to five treatments. The soybeans were grown in SPAR units, and were harvested on July 25th, August 15th, and September 2nd. The treatments applied to the two cultivars are shown in the following table.

SPAR Unit	Day Temperature (°C)	Night Temperature (°C)	Treatment
1	30	22	Control
2	38	30	High Temp
3	22	14	Low Temp
4	30	27.8	High Night Temp
5	30	22	Drought (-50% H_2O)

Results:

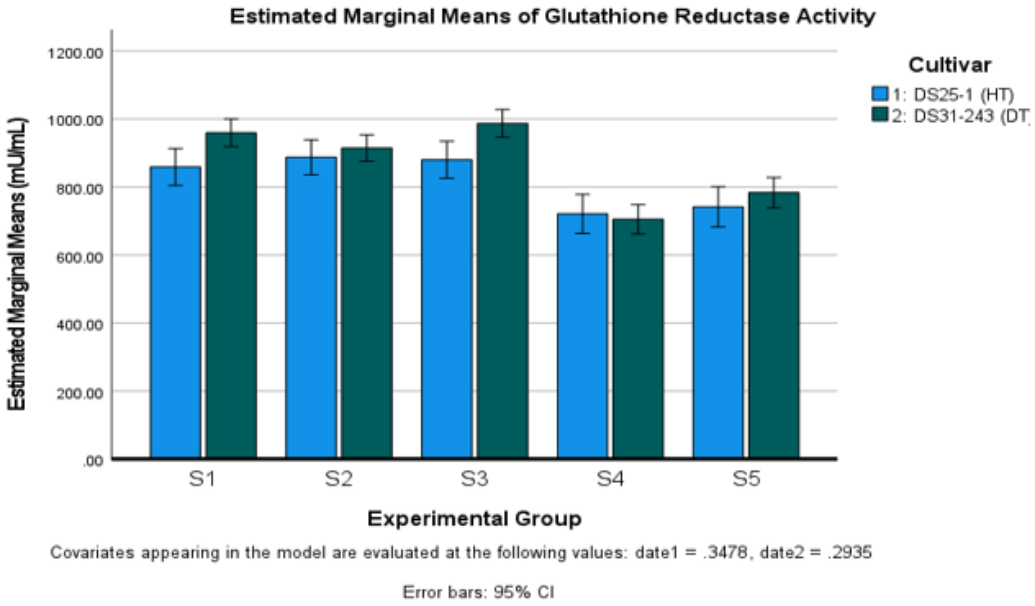

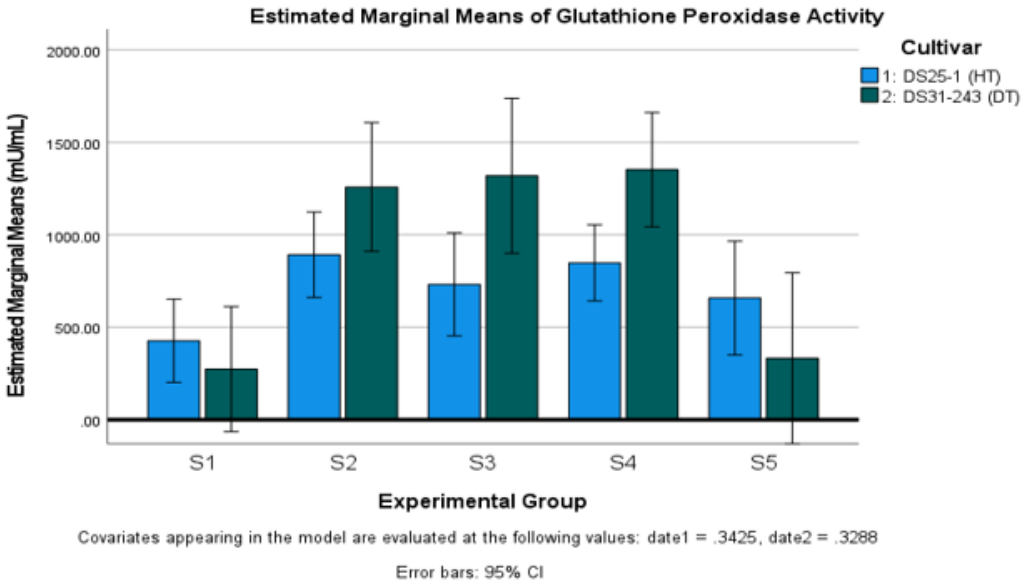
Estimated Marginal Means of Glutathione Peroxidase Activity
Cultivar
1: DS25-1 (HT)
2: DS31-243 (DT)
Estimated Marginal Means (mU/mL)
2000.00
1500.00
1000.00
500.00
.00
S1
S2
S3
S4
S5
Experimental Group
Covariates appearing in the model are evaluated at the following values: date1 = .3425, date2 = .3288
Error bars: 95% CI

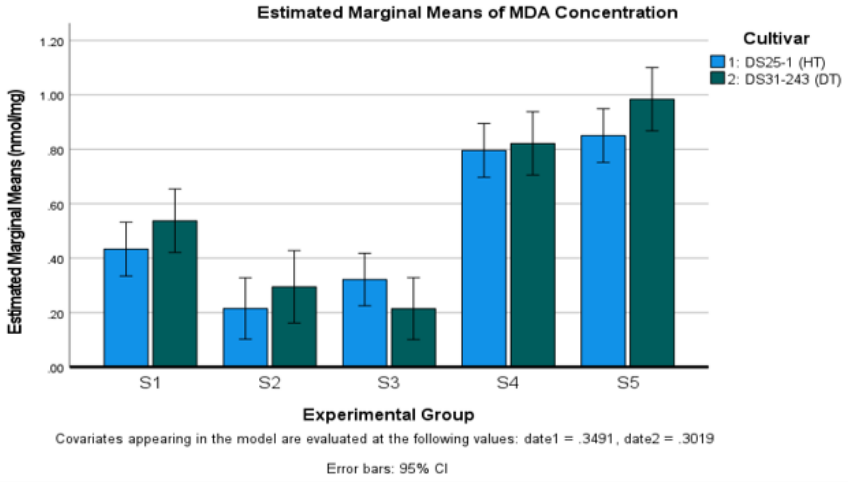
Estimated Marginal Means of MDA Concentration
Cultivar
1: DS25-1 (HT)
2: DS31-243 (DT)
Estimated Marginal Means (nmol/mg)
1.20
1.00
.80
.60
.40
.20
.00
S1
S2
S3
S4
S5
Experimental Group
Covariates appearing in the model are evaluated at the following values: date1 = .3491, date2 = .3019
Error bars: 95% CI

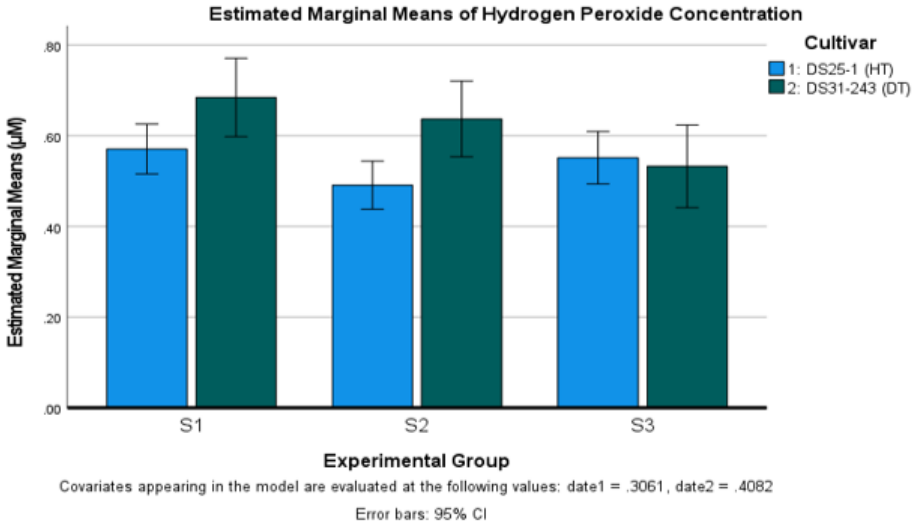

Overall, the experimental group had a statistically significant impact on the ROS-related compounds' concentrations for both cultivars. DS25-1 (HT) exhibited lower concentrations if the experimental conditions were temperature-related, potentially validating resilience to temperature variation.

Future Work:

In the future, the hydrogen peroxide protocol will be applied to the SPAR4 and SPAR5 experimental groups, potentially influencing the conclusions. Dr. Reddy's study included 10 treatments, and S6-10 is currently being assayed.

Name: McKenna Alden

Faculty Mentor: Dr. Adam Skarke

Major: Environmental Geoscience

Department: Geosciences

Teaching Artificial Intelligence (AI) to Recognize Methane Seeps in Water Column Data

Introduction

This past spring, I worked with Dr. Skarke, Surabhi Gupta, and members of the computer engineering department to help teach an AI to recognize methane seeps in water column data. My main role was providing the data to use to teach the AI. Teaching AI to recognize these seeps will help save researchers a lot of time looking through this data as they will not have to go through thousands of individual images looking for these seeps.

Methods

My role in this project was going through thousands of individual images of water column data myself and manually selecting methane seeps using MATLAB. I would scan these images for the seeps. Once I found one, I would use the MATLAB program provided for me to use a box to select where the seep feature was located in the image. Selecting these features would allow the AI to learn what it is looking for in the data. This helped teach me to be familiar with analyzing water column data, using MATLAB, and understanding a little bit more about AI.

Example Image

This image below shows what the water column data that is being analyzed looks like.

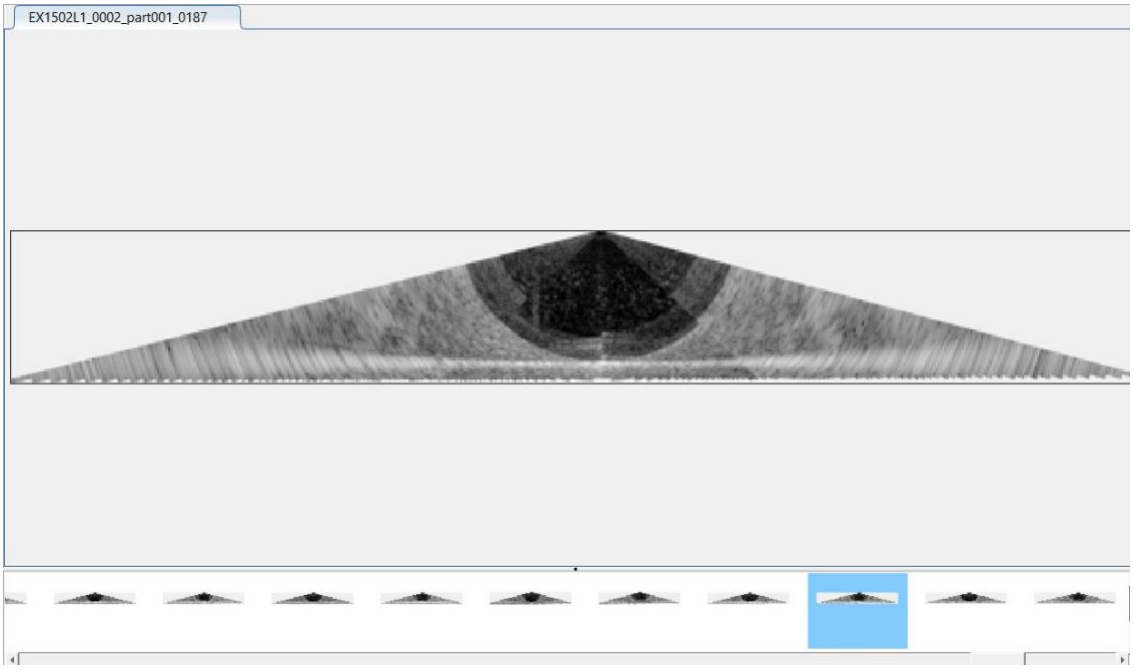

Maggie Phillips

Faculty Mentor: Dr. Matthew K. Ross

Department of Comparative Biomedical Sciences

CES1 Releases Oxylipins from Oxidized Triacylglycerol (oxTAG) and Regulates Macrophage oxTAG/TAG Accumulation and PGE_2/IL-1β Production

Carboxylesterase 1 (CES1) is a serine hydrolase that plays an important role in the metabolism of xenobiotics[1]. Although it has been shown to hydrolyze oxidized triacylglycerols (TAGs), it is unclear which fatty acids are preferentially released through CES1-catalyzed hydrolysis. I began a study in 2021 of the roles of CES1 in macrophages using cell lines with and without the expression of CES1, and I used the support of the Shackouls Research Fellowship for the Spring 2023 semester to complete and publish my work on this project.

This spring, we confirmed our study of CES1 activity in mice and began studying regulatory molecules related to the CES1 lipid metabolism pathways. Using mouse alveolar macrophages from control and CES1 knockout mice, we examined gene expression of lipid regulatory proteins using PCR. We isolated bioactive lipids in mouse lung tissue to determine the lipid environment being studied, and we began a study using Western Blots for the PPARγ concentration in macrophages, which regulate genes involved in lipid metabolism. The results and methods of these studies can be read in greater detail in the manuscript linked at the end of this report.

I used the fellowship funding primarily for wages for 15 hours/week of research in the vet school. Additionally, the fellowship supported the printing of posters for the Mississippi Honors Conference research symposium and the MSU Spring 2023 Undergraduate Research Symposium. Finally, I used the funding to pay the submission fee to *ACS Chemical Biology* for a

manuscript, which was published in June, detailing the activity of CES1 towards TAGs in macrophages. The manuscript is cited and linked below:

Phillips, M. E., Adekanye, O., Borazjani, A., Crow, J. A., & Ross, M. K. (2023). CES1 Releases Oxylipins from Oxidized Triacylglycerol (oxTAG) and Regulates Macrophage oxTAG/TAG Accumulation and PGE_2/IL-1β Production. *ACS chemical biology*, *18*(7), 1564–1581. https://doi.org/10.1021/acschembio.3c00194

https://pubs.acs.org/doi/10.1021/acschembio.3c00194

References:

1. Ross, M. K.; Crow, J. A. Human Carboxylesterases and Their Role in Xenobiotic and Endobiotic Metabolism. *J. Biochem. Mol. Toxicol.* **2007**, *21*, 187– 196, DOI: 10.1002/JBT.20178

Surabhi Gupta

MSU Shackouls Honors College Research Fellowship Project Description

Title: Training and Validation of Machine Learning Algorithms for Automated Detection of Seafloor Gas Seeps.

Introduction:

Seafloor seeps are locations where gas (mostly methane) is discharged from marine sediments into the ocean. They are widely recognized as an important component of the global carbon cycle because they directly link methane (CH4) reserves in subseafloor sediments — the largest carbon reservoir on Earth — to the marine environment. Methane released at seeps drives a wide range of interconnected biogeochemical processes in the shallow subsurface, at the seafloor, and in the overlying water column. These processes contribute to ocean acidification and deoxygenation but also result in extraordinary hotspots of deep-sea benthic biodiversity with unique microbial rock outcrops that harbor complex chemosynthetic ecosystems. Additionally, gas seeps indicate the potential for significant marine geohazards and are a demonstrated energy production resource as well as habitat for commercially viable marine species. Gas seeps are globally distributed, and their discovery has largely been a result of recent large-scale seafloor and water column mapping efforts with advanced multibeam sonar systems on research vessels. Given the relevance of gas seeps to the global carbon cycle, a wide range of oceanographic processes, and economic development of the ocean, their continued discovery is an important ocean exploration priority. However, seep detection currently requires manual visual review and interpretation of water column sonar imagery by a trained individual, which is time consuming, costly, and inconsistent. This often causes delays in new seep discoveries and can result in seeps remaining undiscovered in surveyed areas, because the time and funding necessary to manually identify seeps is prohibitive.

To address this challenge, two researchers (Adam Skarke & Ali Gurbuz) at Mississippi State University are developing a machine learning (ML) based software system to automatically detect gas seeps in water column sonar data. The development of this machine learning software requires an extensive database of water column sonar images in which the presence or absence of a seep signature has been confirmed. The database is first used to train the software to identify seep signatures in sonar data and then later used to evaluate how skilled the software is at making those detections. To generate such a database, it is necessary for an individual, trained in water column sonar interpretation and seep detection, to manually review sonar imagery and tag each image as having a seep signature present or not. Accordingly, for my research project, I will work with Dr. Skarke and his research group to become trained in seep identification in sonar water column data. I will then produce a water column sonar database that will be used to train and validate ML algorithms used for automated seep detection.

Significance:

The project that my research will contribute to will create a broadly applicable ocean exploration technology that will substantially increase the speed, accuracy, and consistency of seafloor gas seep detection, while also decreasing cost and personnel requirements. The resulting discoveries will improve our basic understanding of the quantity and location of seafloor gas seeps around the world. Reducing the gap in our knowledge of seep abundance distribution will directly address pressing scientific questions, inform effective commercial resource management, and support national security priorities. Most notably, given that methane is a potent greenhouse gas and oceanic deposits are the largest reservoir of it, understanding abundance and distribution of gas seeps is of paramount importance for development of accurate models of global carbon cycling and its relationship to climate change. The specific research work I undertake, will directly improve the quality of the automated seep detection system and therefore its ultimate capacity to deliver the broader project outcomes described above.

Methods:

I will undertake the following tasks in the course of my research project:

1. I will become proficient at the use of specialized sonar data processing, analysis, and imaging software (QPS FM Midwater) as well as general data processing software (MATLAB). I will also receive training in relevant geophysics principles (underwater acoustics).

2. I will become proficient in interpretation of water column sonar data and identification of seafloor gas seep features in sonar data. This analysis will include determination of the acoustic backscatter amplitude range and feature shape characteristics indicative of the presence of gas seeps.

3. I will use the software and sonar interpretation proficiency I gain to analyze sonar water column data and tag each sonar image to indicate the presence or absence of seafloor gas seep features. I will also create a database to store the resulting seep identification information and associated sonar data for use in training and validation of automated seep detection algorithms.

4. I will attend regular project meetings with Dr. Skarke's and Dr Gurbuz's research groups and contribute to algorithm development through my gained expertise in interpreting the acoustic signature of seeps in water column sonar data.

5. I will continue to work further on this project and process the data as I did in fall 2022 semester.

An MSU laptop with necessary software and an external data drive has been provided to me.

Surabhi Gupta

MSU Shackouls Honors College Research Fellowship Project Budget

Title: Training and Validation of Machine Learning Algorithms for Automated Detection of Seafloor Gas Seeps

Budget:

A. Personnel $1,980.00

Finds for personnel are requested in the amount of $1980.00 to support the compensation of undergraduate researcher Surabhi Gupta. This compensation is calculated based on an hour rate of $11.00 for work not to exceed 12 hours per week for the duration of the spring 2023 academic semester (see table below). Surabhi Gupta working under the direction of Dr. Skarke will become proficient at the use of specialized sonar data processing, analysis, and imaging software (QPS FM Midwater) as well as general data processing software (MATLAB). She will also become proficient in interpretation of water column sonar data and identification of seafloor gas seep features in sonar data. She will use the resulting proficiency to analyze sonar water column data to indicate the presence or absence of seafloor gas seep features and create a database to store the resulting induration and sonar data for use in machine learning applications. She will contribute her expertise to the development of seep detection algorithms and regularly participate in project meetings with Dr. Skarke's and Dr. Gurbuz's research groups. She will continue to work on this project as more data needs to be processed, which she did for the fall 2022 semester.

Position Title & Name	**Hourly Salary**	**Anticipated Hours Per Week**	**No. of Weeks Jan 16 – May 6, 2023**	**Cost**
Undergraduate Researcher: Surabhi Gupta	$11.00/hr	12	15	$1,980.00
Total Personnel:				**$1,980.00**